RENAL FAILURE
2019, VOL. 41, NO. 1, 455–466
https://doi.org/10.1080/0886022X.2019.1619582

Taylor & Francis
Taylor & Francis Group

LABORATORY STUDY

Niban protein regulates apoptosis in HK-2 cells via caspase-dependent pathway

Shiqi Tang, Jianwen Wang*, Jishi Liu*, Yan Huang, Yueyi Zhou, Shikun Yang, Wei Zhang, Minghui Yang and Hao Zhang

Department of Nephrology, The Third Xiangya Hospital, Central South University, Changsha, China

ABSTRACT

Purpose: To investigate whether Niban protein plays a role in renal interstitial fibrosis by regulating renal tubular epithelial cell apoptosis and explore the underlying mechanism.

Methods: Unilateral ureteral obstruction (UUO) model was performed in C57B/6J mice, and divided into sham operation group and groups of days 3, days 7, and days 14. Niban expression was detected by immunohistochemistry and Western blot. TUNEL assays were used to detected apoptosis. Niban siRNA and overexpression Niban plasmid were transfected in HK-2 cells respectively to explore apoptosis related mechanisms of Niban during angiotensin II (AngII) – and endoplasmic reticulum (ER) stress-induced injury.

Results: With the development of obstruction, Niban's expression decreased gradually while apoptosis increased. Silencing of Niban not only increased the AngII- and ER stress-induced apoptosis, but also promoted the expression of caspase 8, caspase 9, Bip, and Chop. Overexpression of Niban reduced AngII-induced apoptosis and the expression of caspase 8 and caspase 9.

Conclusions: Niban protein is involved in apoptosis regulation in HK-2 cells, and most likely via caspase-dependent pathway.

ARTICLE HISTORY
Received 20 February 2019
Revised 6 May 2019
Accepted 7 May 2019

KEYWORDS
Apoptosis; renal interstitial fibrosis; Niban; chronic kidney disease; unilateral ureteral obstruction

Introduction

Chronic kidney disease (CKD) is increasingly considered a global public health problem [1–3]. Renal interstitial fibrosis (RIF) is the common pathway and the main pathological basis for the progression of various CKDs to end-stage renal disease (ESRD) [4]. The cellular mechanisms leading to renal fibrosis are complex, including inflammation, oxidative stress, apoptosis, and senescence in the form of proximal tubule cell death [5]. A number of studies have shown that cell stress or damage caused by fibrotic stimuli mainly occurs in the renal tubular epithelial compartment, especially the proximal tubule [6,7]. Evidence from the mouse acute kidney injury (AKI) model indicates that apoptosis is more closely related to necrosis than the level of renal insufficiency [8]. Apoptosis can be activated by binding to various death receptors such as Fas/CD95 ligand, tumor necrosis factor (TNF)-α and TNF (ligand) superfamily, members 10 (TNFSF10). Renal tubular cells express these cell surface death receptors, activate caspases in the kidney and initiate apoptosis [9]. Studies have shown that knocking out Bax and Bak genes (pro-apoptotic factors) can block renal tubular cell apoptosis without affecting tubular necrosis, thereby achieving the effect of protecting renal tubular cells [10]. Apoptosis is considered one of the most important mechanisms that promote fibrosis, constituting a research hotspot.

Niban, also termed FAM129A or C1orf24, was originally identified from a rat with renal carcinoma displaying TSC2 gene mutation. It is elevated in animal models and patients with various tumors, playing an important role in regulating gene transcription, protein synthesis, cell proliferation, and apoptosis in tumor cells [11–13]. Our previous study first found that Niban not only regulates apoptosis in tumor cells, but also participates in in the apoptosis of renal tubular epithelial cells, and may be involved in RIF, but the specific mechanism of action remains unclear [14]. Therefore, the present study investigates the mechanism by which Niban alters renal

CONTACT Jishi Liu 26545559@qq.com; Jianwen Wang jwwangdoc@163.com Department of Nephrology, The Third Xiangya Hospital of Central South University, 138 Tongzipo Road, Hunan Province, Changsha 410013, China
*These authors contributed equally to this work.

interstitial fibers by affecting apoptosis in renal tubular epithelial cells.

Methods

Animal model establishment

A total of 24 SPF grade C57BL/6J male mice (18–25 g) were purchased from Hunan Slack Jingda Experimental Animal Limited (Changsha, China). The entire animal study was performed at the Animal Experimental Department of Central South University. Mice were divided into four groups according to the principle of complete randomization, including sham operation animals, and UUO model mice treated at 3, 7, and 14 days. Six mice were caged to provide feed and water without restriction. UUO surgery was performed one week after adaptive feeding, and fasting was started one day before surgery. According to animal weight, 0.3–0.4 mL/100 g of 10% chloral hydrate was intraperitoneally injected. The operation was completed in aseptic conditions. Mice were sacrificed at 3, 7, and 14 days. Half of the obstructed kidney tissue was soaked with 4% formalin, for H&E staining, Masson staining, and immunohistochemistry; the other half of the kidney tissue was stored in liquid nitrogen for subsequent Western blot experiments.

Cell culture experiments

The human proximal renal tubular epithelial HK-2 cells line was purchased from American Type Culture Collections (ATCC, Rockville, MD, USA). HK-2 cells were grown in DMEM/F12 (Gibco, Carlsbad, CA, lot 8117270) supplemented with 10% fetal bovine serum (FBS, BI), 100 U/mL penicillin (Gibco, Carlsbad, CA, BRL), and 100 U/mL streptomycin (Gibco, Carlsbad, CA, BRL), in an incubator containing 5% CO_2 at 37 °C. HK-2 cells were plated in six-well plates the day before staining and treated with OPTI (Gibco, Carlsbad, CA, 1869014). After overnight incubation (50–70% confluency), the cells were transfected with the Niban plasmid and siRNA, respectively, using liposome lip2000 (Invitrogen, Carlsbad, CA, lot1888645). After 5–6 h of incubation as above, serum-free complete culture medium was used to replace the transfection medium. After one day of synchronized culture, the cells were stimulated with AngII (10–6 mol/L) for 48 h, and proteins were collected for Western blot. Using TM (3 μg/mL) to stimulated HK-2 cells for 24 h, proteins were collected for Western blot.

Antibodies and reagents

The Niban plasmid was purchased from Shandong Weizhen Biotechnology Ltd. (Zibo, China) and Vigene Biosciences (Rockville, MD, USA); siRNA was from Guangzhou Ribobio Biological Ltd. (Guangzhou, China). Antibodies against collagens I and III, and α-SMA were purchased from Abcam (Cambridge, UK). Anti-Niban (21333-1-AP); cleaved-caspase 12 (55238-1-AP); b-actin (20536-1-AP); E-cadherin (20874-1-AP); Bip (115871-1-AP); Chop (15204-1-AP); P53 (10442-1-AP) antibodies were obtained from Proteintech (Rosemont, IL). Antibodies targeting cleaved-caspase 3 (CST 9664) were purchased from Cell Signaling Technology (Danvers, MA). Antibodies targeting cleaved-caspase 8 (ab108333) and cleaved-caspase 9 (ab202068) were purchased from Abcam (Cambridge, UK). Anti-AngII antibody was purchased from Santa Cruz (Santa Cruz, CA). Tunicamycin (TM) was purchased from Meilunbio (Nanning, China, MB 5419). Lip2000 was purchased from Invitrogen (Carlsbad, CA).

Immunohistochemistry

Animal tissue samples were embedded in paraffin, and dewaxed (59 °C) and hydrated overnight. Sodium citrate buffer solution was used at boiling for antigen retrieval. After blocking with 1% BSA, primary antibodies (Niban, 1:100; E-cadherin, 1:200; COL I, 1:500; COL III, 1:500) were applied overnight, respectively. Then, secondary antibodies were applied for 1 h. After DAB development, the samples were counterstained with hematoxylin, resin sealed and observed under a microscope.

TUNEL assay

Apoptosis of renal tissue of UUO mouse was measured with terminal deoxynucleotidyl transferase-mediated (dUTP) nick end-labeling (TUNEL) staining (Cell Death Detection Kit, Roche, Penzberg, Germany). Paraffin-embedded tissue was treated in protocols from TUNEL Kit. Slides were developed with DAB and counterstained with 10% hematoxylin in the end. Apoptosis rate analysis was performed by Image-pro plus 6.0 (Media Cybernetics, Inc., Rockville, MD, USA).

Western blot

As described above, protein samples were collected from animal experiments and cell assays for immunoblot. Anti-Niban, E-cadherin, COL I, α-SMA, cleaved-caspase 3, cleaved-caspase 8, cleaved-caspase 9, cleaved-caspase

12, and β-actin primary antibodies were all diluted at 1:1000 and incubated with samples at 4 °C overnight. Development was performed on an Odyssey two-color infrared laser imaging system. The Image J software was used for protein quantification; results are expressed as percentage change in average band density compared to the corresponding control value.

Transfection

Cells were seeded in six-well plates (6×10^5 cells/well) and cultured with OPTI overnight to 50–70% confluency. Then, transfection was performed with siRNA (50 ng/well) and Niban plasmid (4 μg/well) in HK-2 cells using lipo2000 (5 μL/well). After culture with normal serum without antibiotics, the medium was replaced by complete medium after 5–6 h. Then, synchronized cultures were performed for 24 h, and cells were stimulated with AngII (10–6 mol/L) for 48 h. Finally, cell total protein was extracted for subsequent experiments; overexpression and silencing efficiencies were detected by Western blot.

Statistical analysis

Student's *t* test was used for group pair comparisons, while multiple groups were compared by analysis of variance (ANOVA). Each experiment was repeated at least three times with similar results. Statistical analysis was performed by the SPSS 18.0 software (SPSS, Chicago, IL, USA). $p < .05$ was considered statistically significant.

Results

Renal interstitial fibrosis in UUO mouse models

Morphological changes in the obstructed kidney could be observed by the naked eye after 14 days of UUO modeling. Compared with the control group, the UUO group showed significantly enlarged and swollen kidney with brighter surface, thinner cortex, increased amounts of urine, and fluid obstruction (Figure 1(b)). H&E staining, Masson staining, and immunohistochemistry were used to assess interstitial fibrosis in UUO mice. H&E staining was performed respectively in SHM group and UUO group at days 3, 7, and 14, and qualitative damage to the kidney is shown in Figure 1(a). With the extension of UUO modeling time, renal tubular cells gradually shrank, and luminal vacuolization, myofibroblast proliferation, and inflammatory cell accumulation were observed, these pathological changes were most significant at 14 days. At 14 days after UUO, the score of tubulointerstitial injury in mice was significantly higher than that in SHM mice (Figure 1(c)).

Collagen and E-cadherin are effective indicators of fibrosis. Masson staining showed that, compared with SHM control group, collagen expression levels increased with the development of UUO obstruction, and collagen deposition was greater, especially at 14 days, which was consistent with the immunohistochemical results of COL I, COL III, and E-cadherin (Figure 1(a)). In addition, Western blot detecting col I (Figure 1(d)) and E-cadherin (Figure 1(e)) further confirmed the fibrosis induction effect, especially at 14 days in UUO mice.

Expression levels of Niban in UUO mice

Immunohistochemistry and Western blot were used to detect the expression levels of Niban in UUO mice. Immunohistochemical data (Figure 2(a)) showed that Niban in SHM group was significantly expressed, in both glomeruli and renal tubules, but mainly found in renal tubular epithelial cells. With the development of UUO obstruction, Niban expression was gradually decreased. This was consistent with Western blot findings (Figure 2(b)), indicating that Niban levels decreased with the development of renal fibrosis.

Apoptosis in the UUO model

As shown in Figure 3(a), TUNEL assay showed that apoptosis increased gradually with the extension of UUO obstruction time and peaked at seven days. The expression of cleaved-caspase 3 was detected by Western blot in UUO mice, as shown in Figure 3(b,c). Compared with SHM group, the level of cleaved-caspase 3 was significantly increased in UUO group on day 3 and day 7 (both $p < .05$). There was no statistical significance on day 14 ($p > .05$).

Endoplasmic reticulum (ER) stress occurs during the course of UUO-induced renal fibrosis

The expression of Bip, Chop, and P53 in UUO mice was detected by Western blot. As shown in Figure 4, the levels of Bip, Chop, and P53 in UUO group on day 7 were significantly higher than those in SHM group (both $p < .01$); there was no statistical significance on days 3 and 14 ($p > .05$).

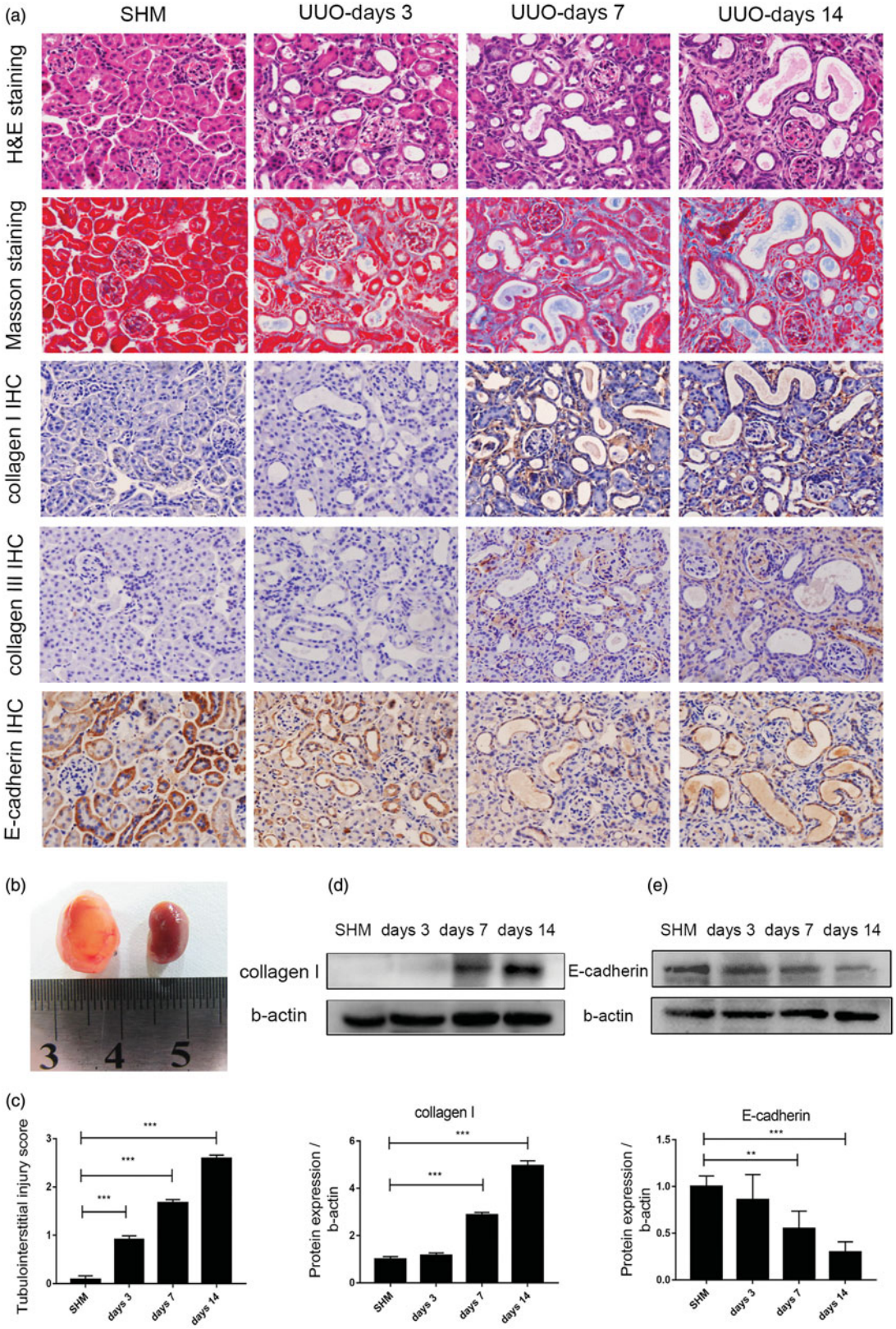

Figure 1. Renal interstitial fibrosis in UUO mouse models. (a) H&E staining of the UUO mouse kidney, Masson staining of the UUO mouse kidney, collagen I, collagen III, and E-cadherin levels detected by immunohistochemistry, the original magnification was ×200 for the H&E, Masson staining, collagen I IHC, collagen III IHC, and E-cadherin IHC. (b) Mouse kidney morphology in the UUO group at days 14 (left) and SHM group (right). (c) Kidney's interstitial lesion scores. (d) Collagen I protein levels by Western blot. (e) E-cadherin protein levels by Western blot. $^{**}p < .01$, $^{***}p < .001$.

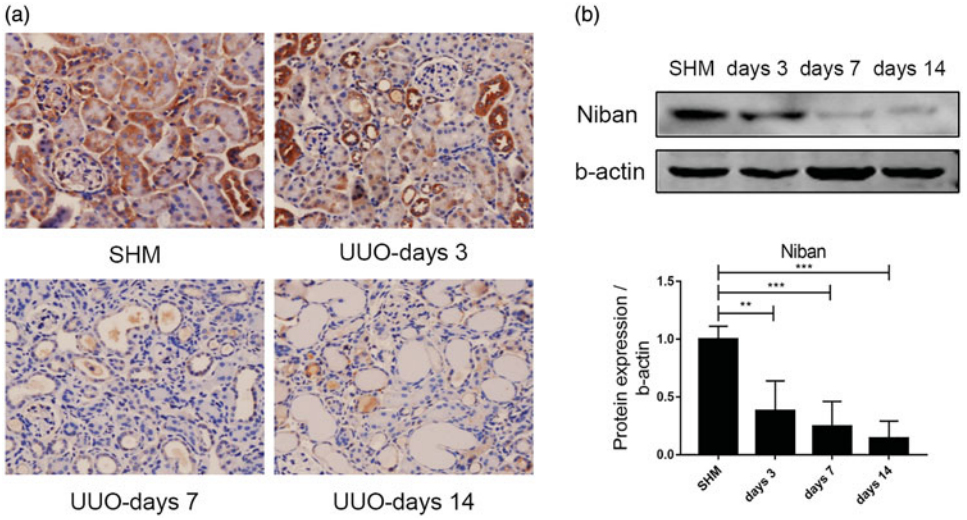

Figure 2. Expression of Niban in UUO mouse models. (a) Niban expression as detected by immunohistochemistry, the original magnification was ×200 for the Niban IHC. (b) Niban expression as assessed by Western blot and quantitation. $^{**}p < .01$, $^{***}p < .001$.

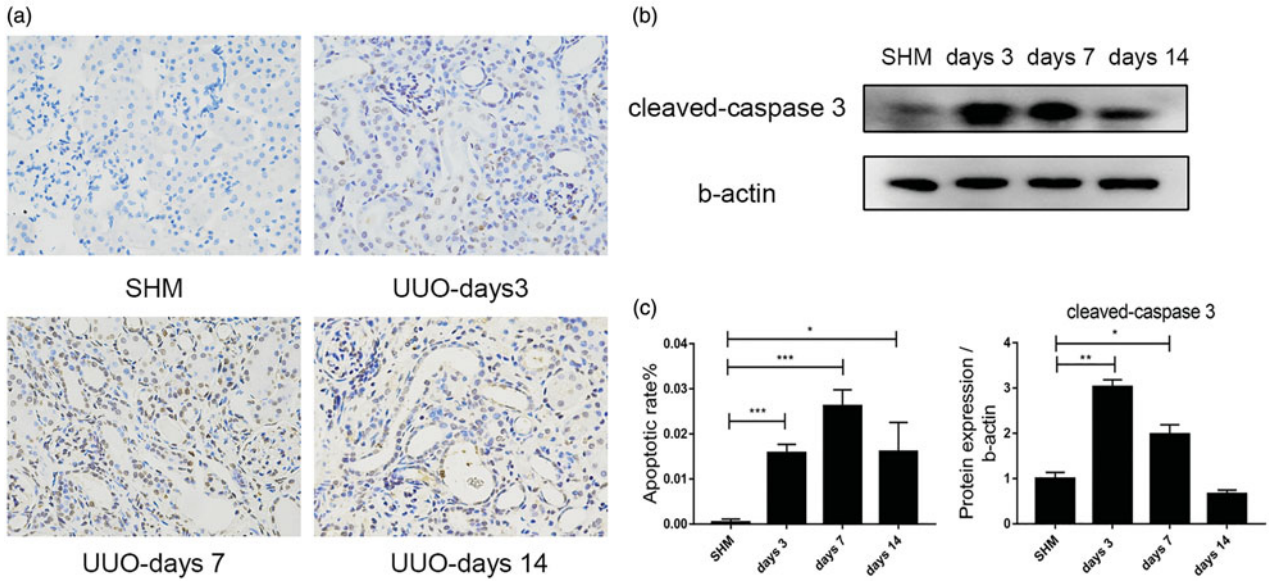

Figure 3. Apoptosis in the UUO mouse models. (a) TUNEL staining data, the original magnification was ×400 for the TUNEL staining. (b) Cleaved-caspase 3 levels determined by Western blot. (c) Apoptotic rates in the TUNEL and relative expression levels of the cleaved-caspase 3 protein. $^{*}p < .05$, $^{**}p < .01$, $^{***}p < .001$.

Expression levels of Niban in HK-2 cells stimulated by AngII

AngII is a common inducer of apoptosis. First, we stimulated HK-2 cells with different concentrations of AngII (10^{-5}, 10^{-6}, and 10^{-7} μmol/L) for 48 h. Then, the expression levels of Niban, E-cadherin, and α-SMA were detected by Western blot (Figure 5(c)). When cells were stimulated with AngII at 10^{-6} μmol/L, the expression levels of Niban and E-cadherin were decreased, while α-SMA expression was increased. Therefore, we selected 10^{-6} μmol/L for subsequent experiments. In order to evaluate the expression of Niban in HK-2 cells and further investigate its role in fibrosis, we silenced Niban by siRNA technology and transfected the overexpressed Niban plasmid, respectively. Then, the cells were stimulated with AngII (10^{-6} μmol/L) to induce apoptosis. After 48 h, the total protein was obtained for Western blot (Niban, E-cadherin, and α-SMA).

Silencing the expression of Niban increased apoptosis and fibrosis in HK-2 cells

As shown in Figure 5(a,b), AngII (10^{-6} μmol/L) stimulated normal HK-2 cells for 48 h, and observed cell

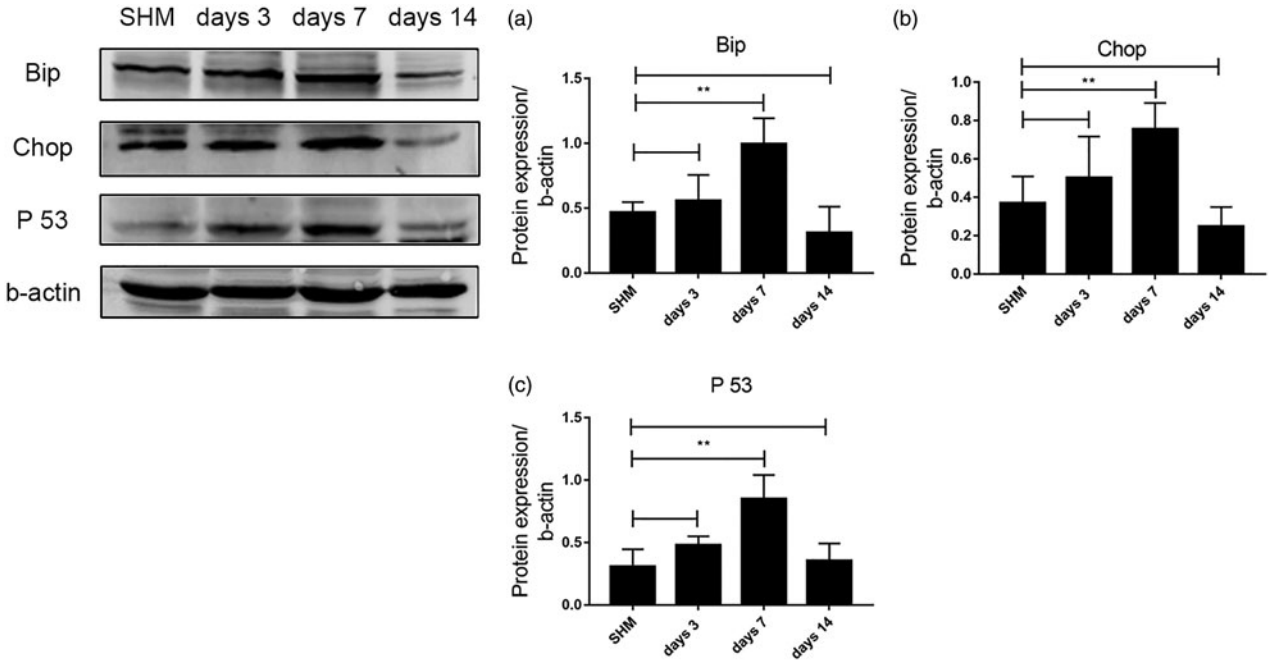

Figure 4. Analysis of P53 and ER stress markers in the kidneys with UUO-induced fibrosis. (a,b) Western blot detection of protein expression levels of Bip and Chop. (c) P53 levels determined by Western blot. $^{**}p < .01$.

morphology under the microscope. HK-2 cells in control group were oval and grew like a paving stone in a six-well plate. After stimulation with AngII, the cells gradually formed a fusiform shape, and overtly long spindles were observed under the microscope. In addition, the cell density was not as high as that of the control group. The Niban siRNA group also had morphological changes, with cells becoming long with stripped spindles, especially, the number of cells in the Niban siRNA + AngII group was significantly lower than that in the control group. The morphology of cells transfected with the Niban plasmid showed no overt changes, even after AngII stimulation, cell morphology was basically elliptical, and cell number was slightly lower than that of the control group ($p > .05$). This may be due to the toxic side effects of the transfection reagent.

After stimulation of HK-2 cells with AngII (10^{-6} μmol/L) for 48 h, the expression levels of Niban and E-cadherin were significantly decreased, while α-SMA expression was markedly increased (all $p < .05$). After Niban silencing, E-cadherin expression was significantly lower than the control group ($p < .01$), while α-SMA levels were significantly increased ($p < .01$). There was no significant difference between the Niban siRNA and Niban siRNA + AngII groups. These results are summarized in Figure 6.

In order to evaluate the role of Niban in regulating the apoptosis of HK-2 cells, we further examined the marker proteins cleaved-caspase 8, cleaved-caspase 9, and cleaved-caspase 12 in three classical apoptotic pathways induced by AngII, including the Fas/FasL pathway, the mitochondrial stress pathway, and ER stress pathway, respectively [15–17]. As shown in Figure 6, the expression levels of cleaved-caspase 8 and cleaved-caspase 9 were increased after stimulation with AngII ($p < .05$). Especially in the Niban siRNA and Niban siRNA + AngII groups, the expression levels of cleaved-caspase 8 and cleaved-caspase 9 were significantly increased ($p < .01$). Meanwhile, there was no significant change in the expression of cleaved-caspase 12 compared with the control group.

Overexpression of Niban reduced apoptosis and relieved renal fibrosis

Compared with the control group, the expression levels of Niban and E-cadherin were decreased after AngII stimulation, while the expression levels of α-SMA were increased (all $p < .05$) (Figure 7). After Niban was transfected into HK-2 cells, its expression was significantly increased compared with that of the control group ($p < .01$). When AngII was used to stimulate HK-2 cells, the levels of Niban, E-cadherin, α-SMA, cleaved-caspase 8, and cleaved-caspase 9 did not change significantly compared with the Niban pENTER group ($p > .05$); cleaved-caspase 12 also showed no changes.

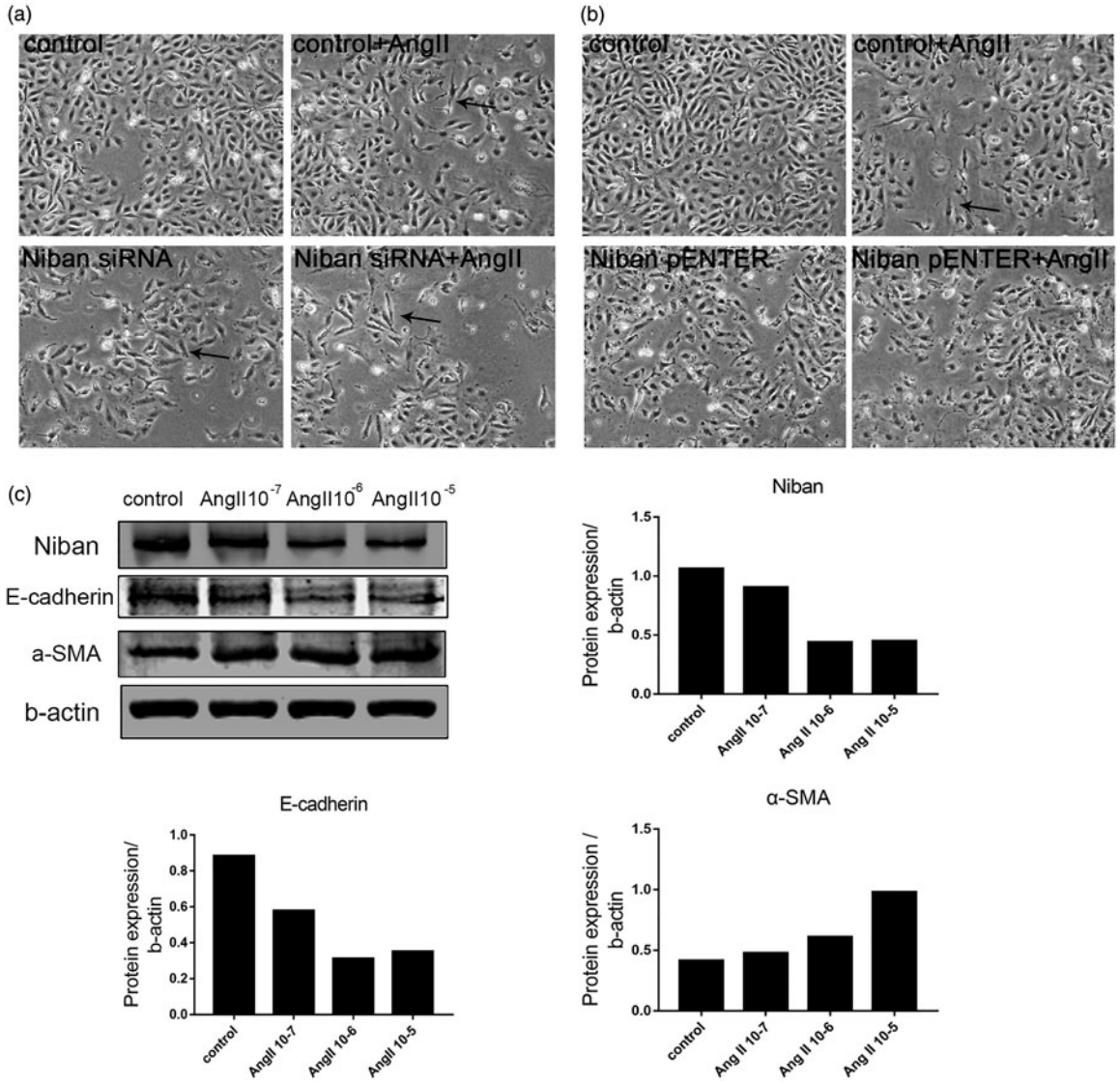

Figure 5. Expression of Niban in HK-2 cells stimulated by AngII. (a,b) Morphology of HK-cells cultured under different treatments, as assessed by electron microscopy, the original magnification was ×200 for the cells. (c) After treatment with different concentrations of AngII to stimulate HK-2 cells, Western blot was used to assess the expression levels of Niban, E-cadherin, and α-SMA.

Silencing the expression of Niban increased endoplasmic reticulum stress

Using TM as an inducer of ER stress; as shown in Figure 8, after stimulation with TM, the expression of Niban in HK-2 cells decreased, while the expression of ER stress marker proteins Bip and Chop was significantly increased ($p < .01$). After inhibiting Niban expression, Bip and Chop of HK-2 cells increased before TM stimulation, but there was no statistical significance ($p > .05$). After TM stimulation, Bip and Chop of HK-2 cells were significantly increased ($p < .001$). When the Niban siRNA + TM group was compared with the control + TM group, Niban decreased ($p < .05$), while the Bip and Chop increased (both $p < .05$).

Discussion

Ureteral obstruction leads to kidney damage and eventually causes irreversible RIF, with extracellular matrix deposition, inflammatory cell infiltration, tubular cell damage, and apoptosis. Apoptosis of renal tubular epithelial cell apoptosis occurs in the early stage of ureteral obstruction. A series of signals, including inflammatory factors and chemokines, are released after cell apoptosis, eventually leading to inflammatory reactions and fibrosis [18,19]. Therefore, inhibiting the early apoptosis of renal tubular cells may prevent the multiple signals from occurring, and thus inhibit the development of fibrosis. The present work aimed to explore new molecular mechanisms, hoping to achieve kidney

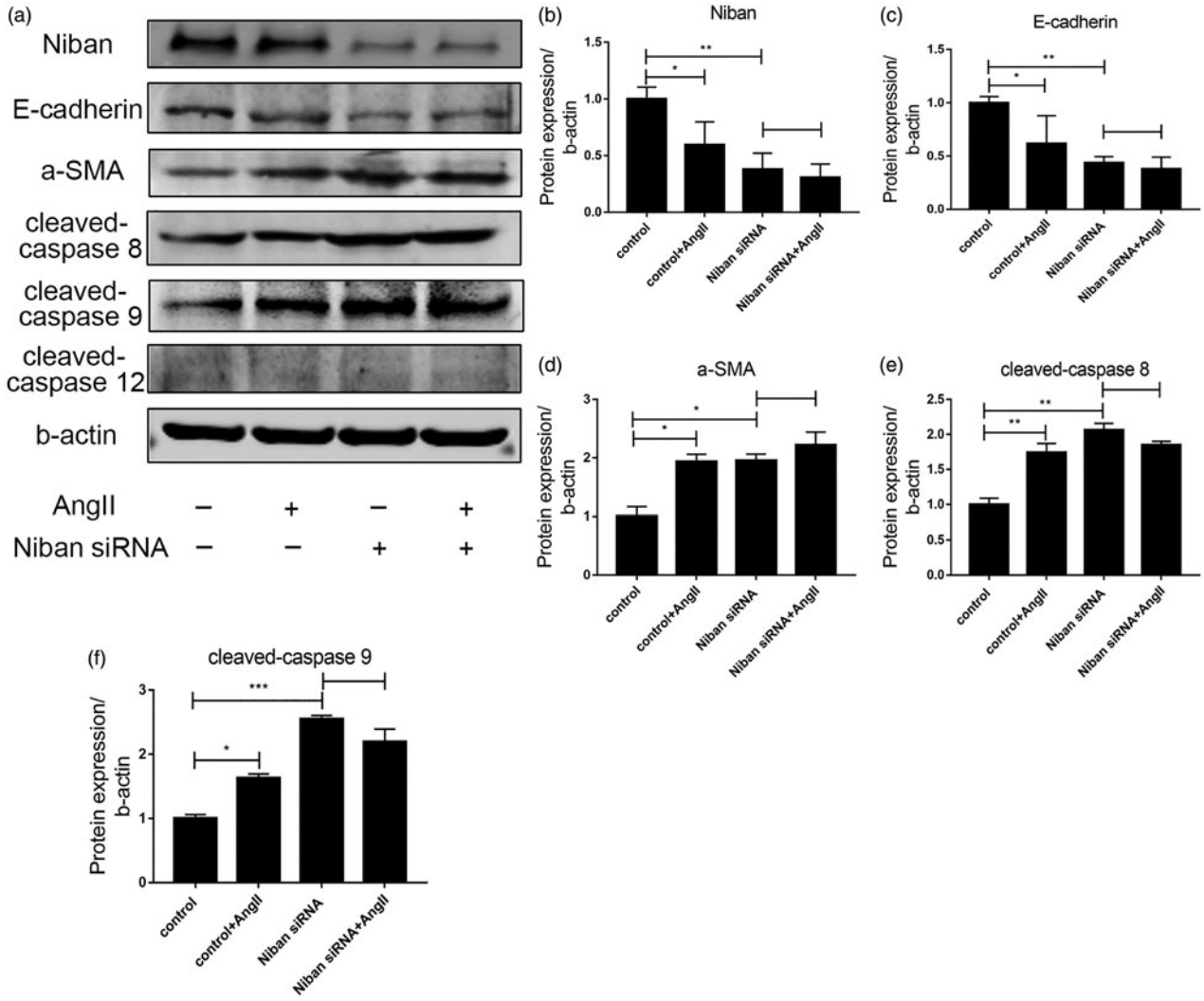

Figure 6. Effect of silencing the expression of Niban. (a) Western blot detection of protein expression levels of Niban, E-cadherin, α-SMA, cleaved-caspase 8, cleaved-caspase 9, and cleaved-caspase 12 in the control, control + AngII, Niban siRNA, and Niban siRNA + AngII groups. (b–f) Relative expression levels of each protein. $^{*}p<.05$, $^{**}p<.01$, $^{***}p<.001$.

protection by regulating apoptosis in renal tubular epithelial cells.

The Niban protein encoded by the FAM129A gene is expressed in various cancers and can inhibit apoptosis [20,21]. Increasing evidence indicates that Niban can not only regulate cell death signals at the transcriptional level to play an inhibitory role in apoptosis [22], but also suppress p53-dependent apoptosis by reducing the formation of NPM–MDM2 complex [23]. In addition, lowering Niban expression can lead to upregulation of p21 and induce apoptosis by inhibiting cell cycle and cell proliferation [24]. Studies have also shown that vasomotor dysfunction leads to decreased phosphorylation of anti-apoptotic protein Niban and promotes apoptosis, while recovery and increase of Niban phosphorylation can upregulate the anti-apoptotic protein Akt and reduce caspase 3/7 activities, restoring vasomotor function and inhibiting apoptosis [25]. Further studies demonstrated that Niban is involved in ER stress and induces autophagy by regulating the mTOR pathway to inhibit apoptosis [22,26]. Due to the anti-apoptotic effect of Niban in various cells, we hypothesize whether Niban plays a role in renal fibrosis by regulating HK-2 cells apoptosis. Our previous study found that Niban is reduced in obstructive nephropathy, UUO rats, as well as in TGF-β1-stimulated HK-2 cells; meanwhile, inhibition of Niban induces apoptosis in HK-2 cells, indicating that Niban may be involved in HK-2 cells apoptosis, but the specific mechanism remains unclear [14].

Apoptosis as a process of regulating cell death, is mainly composed of complex intracellular signal networks. There are three different triggering pathways, including the exogenous (classical death receptor), endogenous (subdivided into mitochondria- and ER stress-induced types) and non-caspase-dependent

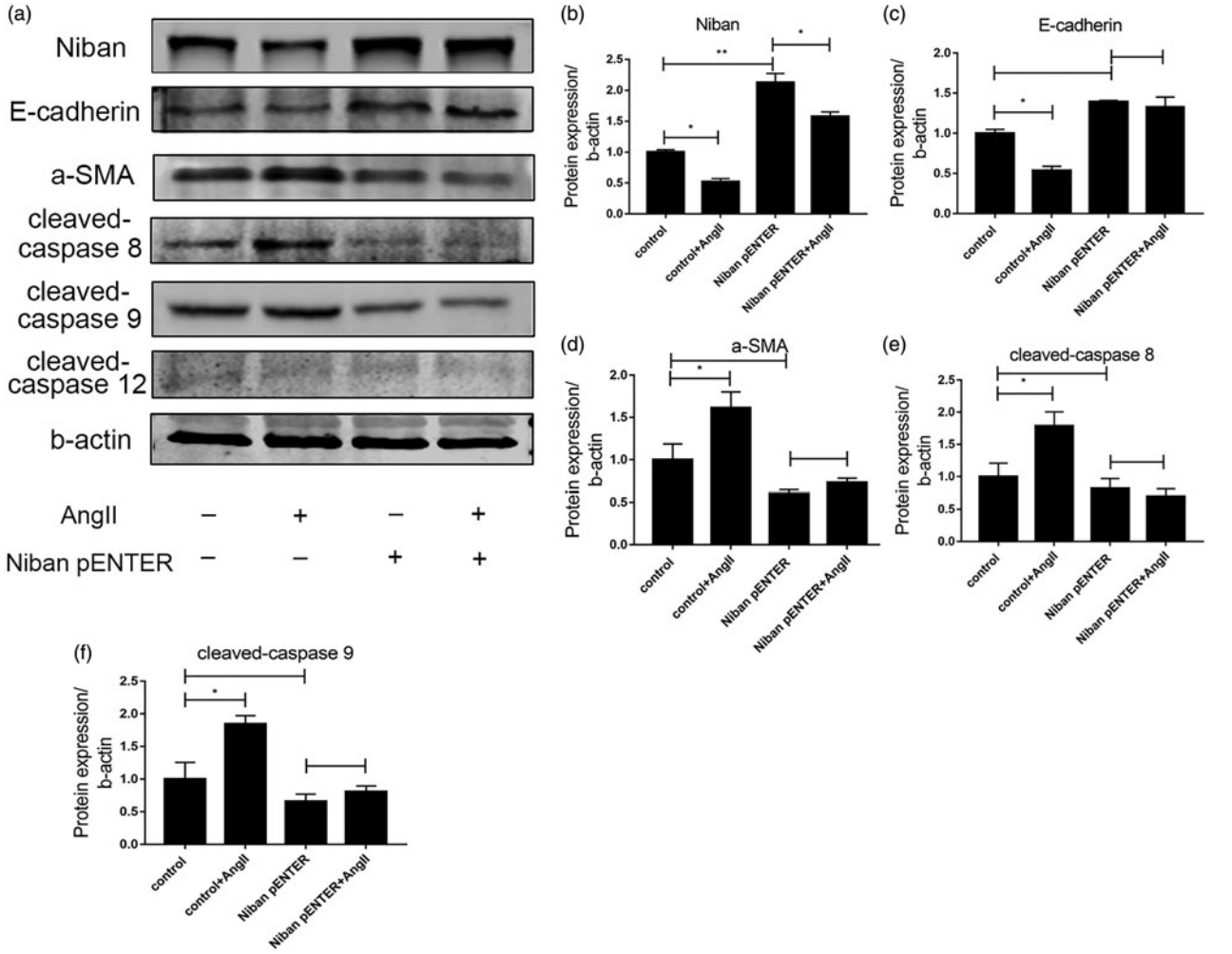

Figure 7. Effect of overexpression of Niban. (a) Western blot for detecting the expression levels of Niban, E-cadherin, α-SMA, cleaved-caspase 8, cleaved-caspase 9, and cleaved-caspase 12 in the control, control + AngII, Niban pENTER, and Niban pENTER + AngII groups. (b–f) Relative expression levels of each protein. $^{*}p<.05$, $^{**}p<.01$.

pathways [27–30]. The Fas/FasL pathway is the most classical death receptor pathway and plays an important role in apoptosis [29,31]. As a marker protein of this pathway, the activation of caspase 8 not only directly triggers apoptosis by activating caspase 3, 6, and 7 (type 1 mechanism), but also induces apoptosis indirectly by activating caspase 9 to stimulate the mitochondrial pathway (type 2 mechanism) [32–34].

In vivo experiments, with the development of UUO obstruction, Niban decreased while apoptosis increased in renal tubular epithelial cells. This result is consistent with our previous UUO rat experiment, suggesting that Niban may be involved in renal tubular epithelial cell apoptosis and thus participate in RIF. As the mechanism is still unclear, we have validated and further explored the results of previous studies. We found that Niban is a functional protein which regulates apoptosis. Our results showed that silencing of Niban up-regulated the levels of cleaved-caspase 8, cleaved-caspase 9, α-SMA, and apoptosis, while down-regulated the level of E-cadherin. Overexpression of Niban down-regulated the level of cleaved-caspase 8, cleaved-caspase 9, α-SMA, and apoptosis, while up-regulated the levels of E-cadherin. Among them caspase 8 and caspase 9 are involved in the Fas/FasL pathway and the mitochondrial stress pathway, respectively, and are marker proteins on these two apoptotic pathways [16,31]. These findings indicated that Niban may inhibit apoptosis in HK-2 cells through caspase-dependent pathway, which is mainly related to the Fas/FasL pathway and the mitochondrial stress pathway. In addition, E-cadherin plays an important role in renal fibrosis as an epithelial marker, α-SMA is a marker protein of myofibroblasts, and it is generally believed that myofibroblasts are the main cell type that produces collagen during fibrosis. References showed that increasing the expression of α-SMA and decreasing the expression of E-cadherin may promote fibrosis [35,36]. Our results showed that

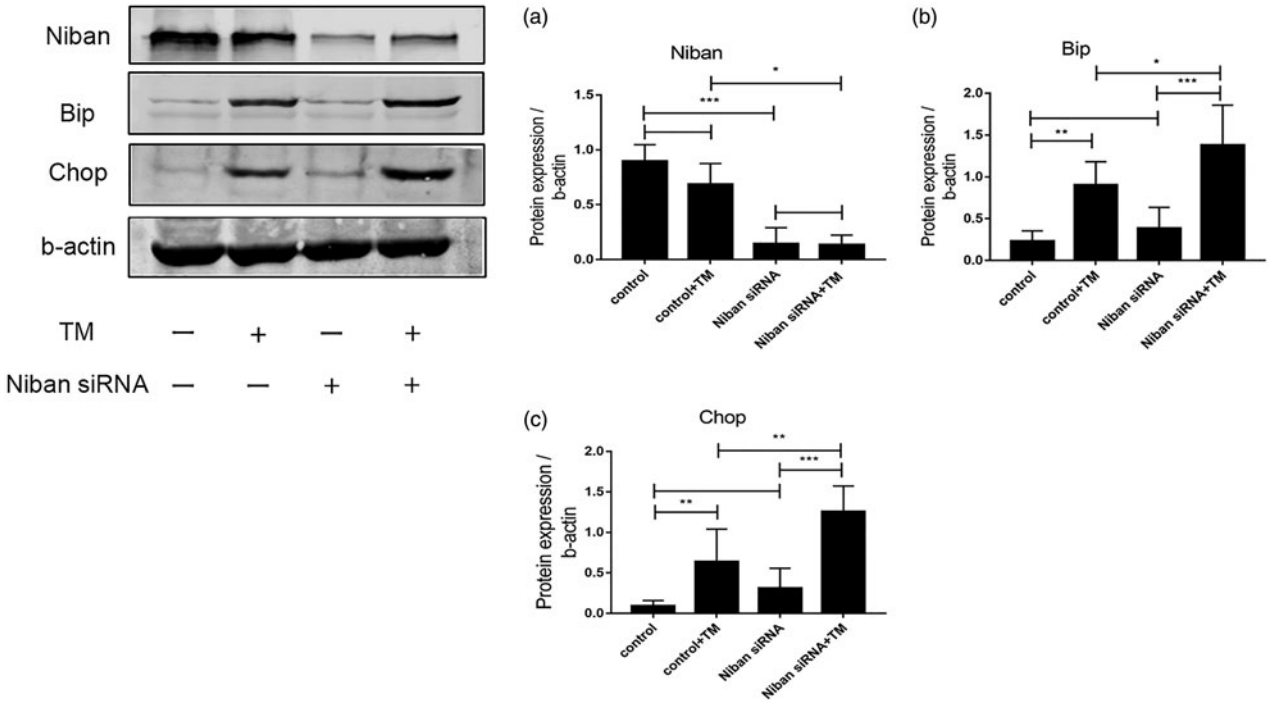

Figure 8. Analysis of ER stress markers in Niban silencing. (a–c) Western blot for detecting the expression levels of Niban, Bip, and Chop. *$p<.05$, **$p<.01$, ***$p<.001$.

overexpression of Niban can reduce AngII-induced apoptosis, decreased expression of α-SMA, and increased expression of E-cadherin. Therefore, we speculated that Niban may relieve fibrosis by inhibiting apoptosis, indicating that Niban may become a new potential target for the treatment of renal fibrosis.

ER stress is a response which multiple stimuli induce the activation of an unfolded protein in the body, which leads to the accumulation of unfolded proteins in the cell, and apoptosis occurs when the stimulation is too severe to be restored by the internal environment. Common ER stress inducers include TM [37–39]. Since caspase12 is involved in the ER stress pathway and is one of its molecular markers [17,30], we examined the marker protein cleaved-caspase 12 of the ER stress pathway. Our results showed that there was no change in the expression of cleaved-caspase 12 after AngII-induced injury. We hypothesize that AngII is not a classical ER stress-inducing factor, but a common inducer of apoptosis. Therefore, AngII induced many other possible apoptotic network pathways, which affected the experimental results.

To investigate whether Niban regulates apoptosis in HK-2 cells through the ER stress pathway, TM was used to stimulate HK-2 cells to detect the marker proteins Bip and Chop of ER stress pathway [37]. We found that after the silencing of Niban, the Bip and Chop of HK-2 cells were significantly increased, especially under the synergistic intervention of TM. The same trend was confirmed in UUO mice, where we found that seven days after UUO modeling, the levels of Bip, Chop, and P53 were significantly increased. P53 is a protein that induces apoptosis. When the damage of the gene is too serious to repair, the p53 protein regulates the repair of cellular DNA and induces apoptosis [40]. These results suggested that silencing the expression of Niban can promote the degree of ER stress in HK-2 cells. Our findings are consistent with the results of Zhang et al. [41], who showed that Chop-related ER stress is associated with the development of renal fibrosis in both CKD patients and unilateral ureteral obstruction (UUO)-induced animals. Studies revealed that loss of Chop protected tubular cells from UUO-induced apoptosis, thereby slowing the progression of renal fibrosis. In view of the role of ER stress in the apoptosis of renal tubular epithelial cells, we speculate that Niban may also regulate the apoptosis of renal tubular epithelial cells by affecting the ER stress pathway.

In summary, our previous study found that Niban plays a role in the apoptosis of renal tubular epithelial cells, which may be involved in RIF, but the specific mechanism of action remains unclear. Based on previous studies, we once again confirmed that Niban is involved in the regulation of HK-2 cells apoptosis. We further discovered that Niban inhibits apoptosis through caspase-dependent pathway, not only via the Fas/FasL and mitochondrial stress pathways, but also ER stress pathways. By regulating these apoptosis

pathways, Niban ultimately affected fibrosis. However, our current mechanism research is mainly focused on the cells level, and Niban knockout mice can be further verified and discussed in the future.

Ethical approval

Animal experiments conform to internationally accepted standards and have been approved by the Ethics Committee of Central South University Department of Laboratory Animals, permit number is 2018sydw0227.

Disclosure statement

No potential conflict of interest was reported by the authors.

Funding

This project was supported by the National Natural Science Foundation of China [81600535] and the National Natural Science Foundation of Hunan Province [2016jj4106].

References

[1] Eckardt KU, Coresh J, Devuyst O, et al. Evolving importance of kidney disease: from subspecialty to global health burden. Lancet (London, England). 2013; 382:158–169.
[2] Levin A, Tonelli M, Bonventre J, et al. Global kidney health 2017 and beyond: a roadmap for closing gaps in care, research, and policy. Lancet (London, England). 2017;390:1888–1917.
[3] Coresh J, Selvin E, Stevens LA, et al. Prevalence of chronic kidney disease in the United States. JAMA. 2007;298:2038–2047.
[4] Hewitson TD. Fibrosis in the kidney: is a problem shared a problem halved? Fibrogenesis Tissue Repair. 2012;5:S14.
[5] Portilla D. Apoptosis, fibrosis and senescence. Nephron Clin Pract. 2014;127:65–69.
[6] Bonventre JV, Yang L. Cellular pathophysiology of ischemic acute kidney injury. J Clin Invest. 2011;121: 4210–4221.
[7] Scott LF, Dean S, Jeremy SD, et al. Therapy for fibrotic diseases nearing the starting line. Sci Transl Med. 2013;5:167sr1.
[8] Havasi A, Borkan SC. Apoptosis and acute kidney injury. Kidney Int. 2011;80:29–40.
[9] Galluzzi L, Vitale I, Abrams JM, et al. Molecular definitions of cell death subroutines: recommendations of the Nomenclature Committee on Cell Death 2012. Cell Death Differ. 2012;19:107–120.
[10] Wei Q, Dong G, Chen JK, et al. Bax and Bak have critical roles in ischemic acute kidney injury in global and proximal tubule-specific knockout mouse models. Kidney Int. 2013;84:138–148.
[11] Majima S, Kajino K, Fukuda T, et al. A novel gene "Niban" upregulated in renal carcinogenesis: cloning by the cDNA-amplified fragment length polymorphism approach. Jpn J Cancer Res. 2000;91:869–874.
[12] Adachi H, Majima S, Kon S, et al. Niban gene is commonly expressed in the renal tumors: a new candidate marker for renal carcinogenesis. Oncogene. 2004;23: 3495–3500.
[13] Okio H. Multistep renal carcinogenesis in the Eker (Tsc 2 gene mutant) rat. Curr Mol Med. 2004;4:807–811.
[14] Liu J, Qin J, Mei W, et al. Expression of Niban in renal interstitial fibrosis. Nephrology (Carlton, Vic). 2014;19: 479–489.
[15] Al-Assaf AH, Alqahtani AM, Alshatwi AA, et al. Mechanism of cadmium induced apoptosis in human peripheral blood lymphocytes: the role of p53, Fas and Caspase-3. Environ Toxicol Pharmacol. 2013;36: 1033–1039.
[16] Yuan Y, Zhang Y, Zhao S, et al. Cadmium-induced apoptosis in neuronal cells is mediated by Fas/FasL-mediated mitochondrial apoptotic signaling pathway. Sci Rep. 2018;8:8837.
[17] Banerjee C, Singh A, Das TK, et al. Ameliorating ER-stress attenuates *Aeromonas hydrophila*-induced mitochondrial dysfunctioning and caspase mediated HKM apoptosis in *Clarias batrachus*. Sci Rep. 2014;4:5820.
[18] Matsuda H, Mori T, Kurumazuka D, et al. Inhibitory effects of T/L-type calcium channel blockers on tubulointerstitial fibrosis in obstructed kidneys in rats. Urology. 2011;77:249.e9–15.
[19] Pang M, Kothapally J, Mao H, et al. Inhibition of histone deacetylase activity attenuates renal fibroblast activation and interstitial fibrosis in obstructive nephropathy. Am J Physiol Renal Physiol. 2009;297:F996–F1005.
[20] Matsumoto F, Fujii H, Abe M, et al. A novel tumor marker, Niban, is expressed in subsets of thyroid tumors and Hashimoto's thyroiditis. Hum Pathol. 2006; 37:1592–1600.
[21] Carvalheira G, Nozima BH, Cerutti JM. microRNA-106b-mediated down-regulation of C1orf24 expression induces apoptosis and suppresses invasion of thyroid cancer. Oncotarget. 2015;6:28357–28370.
[22] Sun GD, Kobayashi T, Abe M, et al. The endoplasmic reticulum stress-inducible protein Niban regulates eIF2alpha and S6K1/4E-BP1 phosphorylation. Biochem Biophys Res Commun. 2007;360:181–187.
[23] Ji H, Ding Z, Hawke D, et al. AKT-dependent phosphorylation of Niban regulates nucleophosmin- and MDM2-mediated p53 stability and cell apoptosis. EMBO Rep. 2012;13:554–560.
[24] Yuki R, Aoyama K, Kubota S, et al. Overexpression of zinc-finger protein 777 (ZNF777) inhibits proliferation at low cell density through down-regulation of FAM129A. J Cell Biochem. 2015;116:954–968.
[25] Luo W, Feldman D, McCallister R, et al. P2X7R antagonism after subfailure overstretch injury of blood vessels reverses vasomotor dysfunction and prevents apoptosis. Purinergic Signal. 2017;13:579–590.
[26] Qaisiya M, Mardesic P, Pastore B, et al. The activation of autophagy protects neurons and astrocytes against bilirubin-induced cytotoxicity. Neurosci Lett. 2017;661: 96–103.

[27] Galluzzi L, Vitale I, Aaronson SA, et al. Molecular mechanisms of cell death: recommendations of the Nomenclature Committee on Cell Death 2018. Cell Death Differ. 2018;25:486–541.
[28] Taylor RC, Cullen SP, Martin SJ. Apoptosis: controlled demolition at the cellular level. Nat Rev Mol Cell Biol. 2008;9:231–241.
[29] Ashkenazi A, Dixit VM. Death receptors: signaling and modulation. Science. 1998;281:1305–1308.
[30] Solano-Galvez SG, Abadi-Chiriti J, Gutierrez-Velez L, et al. Apoptosis: activation and inhibition in health and disease. Med Sci (Basel, Switzerland). 2018;6:pii: E54.
[31] Moradi Marjaneh R, Hassanian SM, Ghobadi N, et al. Targeting the death receptor signaling pathway as a potential therapeutic target in the treatment of colorectal cancer. J Cell Physiol. 2018;233:6538–6549.
[32] Schug ZT, Gonzalvez F, Houtkooper RH, et al. BID is cleaved by caspase-8 within a native complex on the mitochondrial membrane. Cell Death Differ. 2011;18:538–548.
[33] Westphal D, Kluck RM, Dewson G. Building blocks of the apoptotic pore: how Bax and Bak are activated and oligomerize during apoptosis. Cell Death Differ. 2014;21:196–205.
[34] Riedl SJ, Li W, Chao Y, et al. Structure of the apoptotic protease-activating factor 1 bound to ADP. Nature. 2005;434:926–933.
[35] Dong Z, Li S, Wang X, et al. lncRNA GAS5 restrains CCl4-induced hepatic fibrosis by targeting miR-23a through the PTEN/PI3K/Akt signaling pathway. Am J Physiol Gastrointest Liver Physiol. 2019;316:G539–G550.
[36] Zhou H, Gao L, Yu ZH, et al. LncRNA HOTAIR promotes renal interstitial fibrosis by regulating Notch1 pathway via the modulation of miR-124. Nephrology (Carlton, Vic). 2019;24:472–480.
[37] Feng B, Huang X, Jiang D, et al. Endoplasmic reticulum stress inducer tunicamycin alters hepatic energy homeostasis in mice. Int J Mol Sci. 2017;18:pii: E1710.
[38] Song J, Zhang Q, Wang S, et al. Cleavage of caspase-12 at Asp94, mediated by endoplasmic reticulum stress (ERS), contributes to stretch-induced apoptosis of myoblasts. J Cell Physiol. 2018;233:9473–9487.
[39] Sachdev R, Kappes-Horn K, Paulsen L, et al. Endoplasmic reticulum stress induces myostatin high molecular weight aggregates and impairs mature myostatin secretion. Mol Neurobiol. 2018;55:8355–8373.
[40] Wawryk-Gawda E, Chylinska-Wrzos P, Lis-Sochocka M, et al. P53 protein in proliferation, repair and apoptosis of cells. Protoplasma. 2014;251:525–533.
[41] Zhang M, Guo Y, Fu H, et al. Chop deficiency prevents UUO-induced renal fibrosis by attenuating fibrotic signals originated from Hmgb1/TLR4/NFkappaB/IL-1beta signaling. Cell Death Dis. 2015;6:e1847.